Threshold resummation for polarized (semi-)inclusive deep inelastic scattering

Daniele P. Anderle, Felix Ringer, and Werner Vogelsang
Institute for Theoretical Physics, Tübingen University, Auf der Morgenstelle 14, 72076 Tübingen, Germany
(Received 4 April 2013; published 21 May 2013)

We explore the effects of the resummation of large logarithmic perturbative corrections to double-longitudinal spin asymmetries for inclusive and semi-inclusive deep inelastic scattering in fixed-target experiments. We find that the asymmetries are overall rather robust with respect to the inclusion of the resummed higher-order terms. Significant effects are observed at fairly high values of x, where resummation tends to decrease the spin asymmetries. This effect turns out to be more pronounced for semi-inclusive scattering. We also investigate the potential impact of resummation on the extraction of polarized valence quark distributions in dedicated high-x experiments.

DOI: 10.1103/PhysRevD.87.094021 PACS numbers: 12.38.Bx, 13.85.Ni, 13.88.+e

I. INTRODUCTION

Longitudinal double-spin asymmetries in inclusive and semi-inclusive deep inelastic scattering have been prime sources of information on the nucleon's spin structure for several decades. They may be used to extract the helicity parton distributions of the nucleon,

$$\Delta f(x, Q^2) \equiv f^+(x, Q^2) - f^-(x, Q^2), \tag{1}$$

where f^+ and f^- are the distributions of parton $f = q, \bar{q}, g$ with positive and negative helicity, respectively, when the parent nucleon has positive helicity. x denotes the momentum fraction of the parton and Q the hard scale at which the distribution is probed. Inclusive polarized deep inelastic scattering (DIS), $\vec{\ell}\,\vec{p} \to \ell X$, offers access to the combined quark and antiquark distributions for a given flavor, $\Delta q + \Delta\bar{q}$, whereas in semi-inclusive deep inelastic scattering (SIDIS), $\vec{\ell}\,\vec{p} \to \ell h X$, one exploits the fact that a produced hadron h (like a π^+) may for instance have a quark of a certain flavor as a valence quark, but not the corresponding antiquark [1]. In this way, it becomes possible to separate quark and antiquark distributions in the nucleon from one another, as well as to better determine the distributions for the various flavors. HERMES [2] and recent COMPASS [3] measurements have marked significant progress concerning the accuracy and kinematic coverage of polarized SIDIS measurements. The inclusive measurements have improved vastly as well [4–8]. Some modern analyses of spin-dependent parton distributions include both inclusive and semi-inclusive data [9–11]. In addition, high-precision data for polarized SIDIS will become available from experiments to be carried out at the Jefferson Lab after the CEBAF upgrade to a 12 GeV beam [12]. Here the focus will be on the large-x regime.

A good understanding of the theoretical framework for the description of spin asymmetries in lepton scattering is vital for a reliable extraction of polarized parton distributions. In a recent paper [13] we have investigated the effects of QCD threshold resummation on hadron multiplicities in SIDIS in the HERMES and COMPASS kinematic regimes. SIDIS is characterized by two scaling variables: Bjorken-x and a variable z given by the energy of the produced hadron over the energy of the virtual photon in the target rest frame. Large logarithmic corrections to the SIDIS cross section arise when the corresponding partonic variables become large, corresponding to scattering near a phase-space boundary, where real-gluon emission is suppressed. This is typically the case for the presently relevant fixed-target kinematics. Threshold resummation addresses these logarithms to all orders in the strong coupling. In Ref. [13] we found fairly significant resummation effects on the spin-averaged multiplicities. Since the spin-dependent cross section is subject to similar logarithmic corrections as the unpolarized one, it is worthwhile to explore the effects of resummation on the spin asymmetries. This is the goal of the present paper. Our calculations will be carried out both for inclusive DIS and for SIDIS. We note that previous work [14,15] has addressed the large-x resummation for the inclusive spin-dependent structure function g_1, with a focus on the moments of g_1 and their Q^2 dependence. In this paper we are primarily concerned with spin asymmetries and with semi-inclusive scattering.

Our work will use the framework developed in Ref. [13]. In Sec. II, we briefly review the basic terms and definitions relevant for longitudinal spin asymmetries, and we describe the extension of threshold resummation to the polarized case. In Sec. III our phenomenological results are presented. We compare our resummed inclusive and semi-inclusive spin asymmetries with available HERMES, COMPASS and Jefferson Lab data. We also discuss the relevance of resummation for the extraction of $\Delta u/u$ and $\Delta d/d$ at large values of x.

II. RESUMMATION FOR LONGITUDINAL SPIN ASYMMETRIES IN DIS AND SIDIS

A. Leading- and next-to-leading-order expressions

We first consider the polarized SIDIS process $\vec{\ell}(k)\vec{p}(P) \to \ell(k')h(P_h)X$ with a longitudinally polarized beam and target and with an unpolarized hadron in the final state. The corresponding double-spin asymmetry is given by a ratio of structure functions [2],

$$A_1^h(x,z,Q^2) \approx \frac{g_1^h(x,z,Q^2)}{F_1^h(x,z,Q^2)}, \tag{2}$$

where $Q^2 = -q^2$ with q the momentum of the virtual photon, $x = Q^2/(2P \cdot q)$ is the usual Bjorken variable, and $z \equiv P \cdot P_h / P \cdot q$ the corresponding hadronic scaling variable associated with the fragmentation process.

Using factorization, the polarized structure function g_1^h, which appears in the numerator of Eq. (2), can be written as

$$2g_1^h(x,z,Q^2) = \sum_{f,f'=q,\bar{q},g} \int_x^1 \frac{d\hat{x}}{\hat{x}} \int_z^1 \frac{d\hat{z}}{\hat{z}} \Delta f\left(\frac{x}{\hat{x}}, \mu^2\right) \times D_{f'}^h\left(\frac{z}{\hat{z}}, \mu^2\right) \Delta\mathcal{C}_{f'f}\left(\hat{x}, \hat{z}, \frac{Q^2}{\mu^2}, \alpha_s(\mu^2)\right), \tag{3}$$

where $\Delta f(\xi, \mu^2)$ denotes the polarized distribution function for parton f of Eq. (1), whereas $D_{f'}^h(\zeta, \mu^2)$ is the corresponding fragmentation function for parton f' going to the observed hadron h. The $\Delta\mathcal{C}_{f'f}$ are spin-dependent coefficient functions. We have set all factorization and renormalization scales equal and collectively denoted them by μ. In Eq. (3) $\hat{x}$ and $\hat{z}$ are the partonic counterparts of the hadronic variables x and z. Setting for simplicity $\mu = Q$, we use the shorthand notation

$$2g_1^h(x,z,Q^2) \equiv \sum_{f,f'=q,\bar{q},g} [\Delta f \otimes \Delta\mathcal{C}_{f'f} \otimes D_{f'}^h](x,z,Q^2) \tag{4}$$

for the convolutions in Eq. (3). A corresponding expression for the "transverse" unpolarized structure function $2F_1^h$ can be written by replacing the polarized parton distributions with the unpolarized ones, and using unpolarized coefficient functions which we denote here by $\mathcal{C}_{f'f}$.

The spin-dependent hard-scattering coefficient functions $\Delta\mathcal{C}_{f'f}$ in Eq. (3) can be computed in perturbation theory,

$$\Delta\mathcal{C}_{f'f} = \Delta C_{f'f}^{(0)} + \frac{\alpha_s(\mu^2)}{2\pi} \Delta C_{f'f}^{(1)} + \mathcal{O}(\alpha_s^2). \tag{5}$$

At leading order, we have

$$\Delta\mathcal{C}_{qq}(\hat{x},\hat{z}) = \Delta\mathcal{C}_{\bar{q}\bar{q}}(\hat{x},\hat{z}) = e_q^2 \delta(1-\hat{x})\delta(1-\hat{z}), \tag{6}$$

with the quark's fractional charge e_q. All other coefficient functions vanish. The same result holds for the leading order coefficient function for the spin-averaged structure function $2F_1^h$. Hence the asymmetry in Eq. (2) reduces to

$$A_1^h = \frac{\sum_q e_q^2[\Delta q(x,Q^2) D_q^h(z,Q^2) + \Delta\bar{q}(x,Q^2) D_{\bar{q}}^h(z,Q^2)]}{\sum_q e_q^2[q(x,Q^2) D_q^h(z,Q^2) + \bar{q}(x,Q^2) D_{\bar{q}}^h(z,Q^2)]}. \tag{7}$$

At next-to-leading order (NLO), Eq. (3) becomes

$$\begin{aligned} 2g_1^h(x,z,Q^2) = \sum_q e_q^2 \Big\{ & \Delta q(x,Q^2) D_q^h(z,Q^2) \\ & + \Delta\bar{q}(x,Q^2) D_{\bar{q}}^h(z,Q^2) \\ & + \frac{\alpha_s(Q^2)}{2\pi} [(\Delta q \otimes D_q^h + \Delta\bar{q} \otimes D_{\bar{q}}^h) \otimes \Delta C_{qq}^{(1)} \\ & + (\Delta q + \Delta\bar{q}) \otimes \Delta C_{gq}^{(1)} \otimes D_g^h \\ & + \Delta g \otimes \Delta C_{qg}^{(1)} \otimes (D_q^h + D_{\bar{q}}^h)](x,z,Q^2) \Big\}, \end{aligned} \tag{8}$$

where the symbol $\otimes$ denotes the convolution defined in Eqs. (3) and (4). The explicit expressions for the spin-dependent NLO coefficients $\Delta C_{f'f}^{(1)}$ have been derived in Refs. [16,17]. The corresponding spin-averaged NLO coefficient functions $C_{f'f}^{(1)}$ may be found in Refs. [13,16–21].

In the case of *inclusive* polarized DIS, the longitudinal spin asymmetry A_1 is given in analogy with Eq. (2) by

$$A_1(x,Q^2) \approx \frac{g_1(x,Q^2)}{F_1(x,Q^2)}. \tag{9}$$

The inclusive structure functions g_1 and F_1 have expressions analogous to their SIDIS counterparts, except for the fact that they do not contain any fragmentation functions, of course. The unpolarized and polarized NLO coefficient functions for inclusive DIS may be found in many places; see, for example, Refs. [20,22].

B. Threshold resummation

As was discussed in Ref. [13], the higher-order terms in the spin-averaged SIDIS coefficient function $\mathcal{C}_{qq}$ introduce large terms near the "partonic threshold" $\hat{x} \to 1$, $\hat{z} \to 1$. The same is true for the spin-dependent $\Delta\mathcal{C}_{qq}$. At NLO, choosing again for simplicity the scale $\mu = Q$, one has

$$\begin{aligned} \Delta C_{qq}^{(1)}(\hat{x},\hat{z}) \sim e_q^2 C_F \Big[& +2\delta(1-\hat{x}) \left(\frac{\ln(1-\hat{z})}{1-\hat{z}}\right)_+ \\ & + 2\delta(1-\hat{z}) \left(\frac{\ln(1-\hat{x})}{1-\hat{x}}\right)_+ \\ & + \frac{2}{(1-\hat{x})_+(1-\hat{z})_+} \\ & - 8\delta(1-\hat{x})\delta(1-\hat{z}) \Big], \end{aligned} \tag{10}$$

where the "+"-distribution is defined as usual. The expression on the right-hand side is in fact identical to the one for the unpolarized coefficient function near threshold [13]. At the kth order of perturbation theory, the coefficient function contains terms of the form $\alpha_s^k \delta(1-\hat{x}) \times (\frac{\ln^{2k-1}(1-\hat{z})}{1-\hat{z}})_+$, $\alpha_s^k \delta(1-\hat{z})(\frac{\ln^{2k-1}(1-\hat{x})}{1-\hat{x}})_+$, or "mixed" distributions $\alpha_s^k (\frac{\ln^m(1-\hat{x})}{1-\hat{x}})_+ (\frac{\ln^n(1-\hat{z})}{1-\hat{z}})_+$ with $m + n = 2k - 2$, plus terms less singular by one or more logarithms. Again, each of these terms will appear equally in the unpolarized and in the polarized coefficient function. The reason for this is that the terms are associated with the emission of soft gluons [13], which does not care about spin. Threshold resummation addresses the large logarithmic terms to all orders in the strong coupling. The resummation for the case of SIDIS was carried out in Ref. [13]. Given these results and the equality of the spin-averaged and spin-dependent coefficient functions near threshold, it is relatively straightforward to perform the resummation for the polarized case. Having the resummation for both g_1^h and F_1^h, we obtain resummed predictions for the experimentally relevant spin asymmetry A_1^h.

In Refs. [13,23,24] threshold resummation for SIDIS was derived using an eikonal approach, for which exponentiation of the threshold logarithms is achieved in Mellin space. One takes Mellin moments of g_1^h separately in the two independent variables x and z [18,25],

$$\tilde{g}_1^h(N, M, Q^2) \equiv \int_0^1 dx x^{N-1} \int_0^1 dz z^{M-1} g_1^h(x, z, Q^2). \quad (11)$$

With this definition, Eq. (4) takes the form (again at scale $\mu = Q$)

$$2\tilde{g}_1^h(N, M, Q^2) = \sum_{f,f'=q,\bar{q},g} \Delta\tilde{f}^N(Q^2)\Delta\tilde{\mathcal{C}}_{f'f}(N, M, \alpha_s(Q^2)) \times \tilde{D}_{f'}^{h,M}(Q^2), \quad (12)$$

where the moments of the polarized parton distributions and the fragmentation functions are defined as

$$\begin{aligned} \Delta\tilde{f}^N(Q^2) &\equiv \int_0^1 dx x^{N-1}\Delta f(x, Q^2), \\ \tilde{D}_{f'}^{h,M}(Q^2) &\equiv \int_0^1 dz z^{M-1} D_{f'}^h(z, Q^2), \end{aligned} \quad (13)$$

and the double Mellin moments of the polarized coefficient functions are

$$\Delta\tilde{\mathcal{C}}_{f'f}(N, M, \alpha_s(Q^2)) \equiv \int_0^1 d\hat{x}\hat{x}^{N-1} \int_0^1 d\hat{z}\hat{z}^{M-1}\Delta\mathcal{C}_{f'f}(\hat{x}, \hat{z}, 1, \alpha_s(Q^2)). \quad (14)$$

Large $\hat{x}$ and $\hat{z}$ in $\Delta\mathcal{C}_{f'f}$ correspond to large N and M in $\Delta\tilde{\mathcal{C}}_{f'f}$, respectively.

The resummed spin-dependent coefficient function is identical to the spin-averaged one of Ref. [13] and reads to next-to-leading logarithmic (NLL) accuracy in the $\overline{\text{MS}}$-scheme

$$\Delta\tilde{\mathcal{C}}_{qq}^{\text{res}}(N, M, \alpha_s(Q^2)) = e_q^2 H_{qq}(\alpha_s(Q^2)) \times \exp\left[2\int_{\frac{Q^2}{\bar{N}\bar{M}}}^{Q^2} \frac{dk_\perp^2}{k_\perp^2} A_q(\alpha_s(k_\perp^2)) \times \ln\left(\frac{k_\perp}{Q}\sqrt{\bar{N}\bar{M}}\right)\right], \quad (15)$$

where $\bar{N} \equiv N e^{\gamma_E}$, $\bar{M} \equiv M e^{\gamma_E}$, with γ_E the Euler constant, and

$$A_q(\alpha_s) = \frac{\alpha_s}{\pi} A_q^{(1)} + \left(\frac{\alpha_s}{\pi}\right)^2 A_q^{(2)} + \cdots \quad (16)$$

is a perturbative function. The coefficients required to NLL read

$$A_q^{(1)} = C_F, \qquad A_q^{(2)} = \frac{1}{2}C_F\left[C_A\left(\frac{67}{18} - \frac{\pi^2}{6}\right) - \frac{5}{9}N_f\right], \quad (17)$$

where $C_F = 4/3$, $C_A = 3$ and N_f is the number of active flavors. Furthermore,

$$H_{qq}(\alpha_s) = 1 + \frac{\alpha_s}{2\pi}C_F\left(-8 + \frac{\pi^2}{3}\right) + \mathcal{O}(\alpha_s^2). \quad (18)$$

The explicit NLL expansion of the exponent in Eq. (15) is given by [13]

$$\int_{\frac{Q^2}{\bar{N}\bar{M}}}^{Q^2} \frac{dk_\perp^2}{k_\perp^2} A_q(\alpha_s(k_\perp^2)) \ln\left(\frac{k_\perp}{Q}\sqrt{\bar{N}\bar{M}}\right) \approx h_q^{(1)}\left(\frac{\lambda_{NM}}{2}\right)\frac{\lambda_{NM}}{2b_0\alpha_s(\mu^2)} + h_q^{(2)}\left(\frac{\lambda_{NM}}{2}, \frac{Q^2}{\mu^2}, \frac{Q^2}{\mu_F^2}\right), \quad (19)$$

where

$$\begin{aligned} \lambda_{NM} &\equiv b_0\alpha_s(\mu^2)(\log\bar{N} + \log\bar{M}), \\ h_q^{(1)}(\lambda) &= \frac{A_q^{(1)}}{2\pi b_0\lambda}[2\lambda + (1 - 2\lambda)\ln(1 - 2\lambda)], \\ h_q^{(2)}\left(\lambda, \frac{Q^2}{\mu^2}, \frac{Q^2}{\mu_F^2}\right) &= -\frac{A_q^{(2)}}{2\pi^2 b_0^2}[2\lambda + \ln(1 - 2\lambda)] \\ &\quad + \frac{A_q^{(1)}b_1}{2\pi b_0^3}\left[2\lambda + \ln(1 - 2\lambda) + \frac{1}{2}\ln^2(1 - 2\lambda)\right] \\ &\quad + \frac{A_q^{(1)}}{2\pi b_0}[2\lambda + \ln(1 - 2\lambda)]\ln\frac{Q^2}{\mu^2} \\ &\quad - \frac{A_q^{(1)}}{\pi b_0}\lambda\ln\frac{Q^2}{\mu_F^2}, \end{aligned} \quad (20)$$

with

$$\begin{aligned} b_0 &= \frac{11C_A - 4T_R N_f}{12\pi}, \\ b_1 &= \frac{17C_A^2 - 10C_A T_R N_f - 6C_F T_R N_f}{24\pi^2}. \end{aligned} \quad (21)$$

The functions $h_q^{(1)}$, $h_q^{(2)}$ collect all leading-logarithmic and NLL terms in the exponent, which are of the form $\alpha_s^k \ln^n\bar{N}\ln^m\bar{M}$ with $n + m = k + 1$ and $n + m = k$, respectively. Note that we have restored the full dependence on the factorization and renormalization scales in the above expressions.

The polarized moment-space structure function $\tilde{g}_1^{h,\text{res}}$ resummed to NLL is obtained by inserting the resummed coefficient function into Eq. (12). To get the physical hadronic structure function $g_1^{h,\text{res}}$ one needs to take the

Mellin inverse of the moment-space expression. As in Ref. [13], we choose the required integration contours in complex N, M space according to the *minimal prescription* of Ref. [26], in order to properly deal with the singularities arising from the Landau pole due to the divergence of the perturbative running strong coupling constant α_s at scale Λ_{QCD}. Moreover, we match the resummed $g_1^{h,\mathrm{res}}$ to its NLO value, i.e., we subtract the $\mathcal{O}(\alpha_s)$ expansion from the resummed expression and add the full NLO result,

$$g_1^{h,\mathrm{match}} \equiv g_1^{h,\mathrm{res}} - g_1^{h,\mathrm{res}}|_{\mathcal{O}(\alpha_s)} + g_1^{h,\mathrm{NLO}}. \tag{22}$$

The final resummed and matched expression for the spin asymmetry A_1^h is then given by

$$A_1^{h,\mathrm{res}}(x, z, Q^2) \equiv \frac{g_1^{h,\mathrm{match}}(x, z, Q^2)}{F_1^{h,\mathrm{match}}(x, z, Q^2)}. \tag{23}$$

Similar considerations can be made for inclusive DIS, where again the resummation for g_1 proceeds identically to that of F_1 in moment space. Only single Mellin moments of the structure function have to be taken,

$$\tilde{g}_1(N, Q^2) \equiv \int_0^1 dx x^{N-1} g_1(x, Q^2). \tag{24}$$

The threshold resummed coefficient function is the same as in the spin-averaged case and is discussed for example in Ref. [13]. We note that the outgoing quark in the process $\gamma^* q \to q$ remains "unobserved" in inclusive DIS. At higher orders this is known to generate Sudakov *suppression* effects [27] that counteract the Sudakov enhancement associated with soft-gluon radiation from the initial quark. This is in contrast to SIDIS, where the outgoing quark fragments and hence is "observed," so that both the initial and the final quark contribute to Sudakov enhancement. As a result, resummation effects are generally larger in SIDIS than in DIS, for given kinematics.

III. PHENOMENOLOGICAL RESULTS

We now analyze numerically the impact of threshold resummation on the semi-inclusive and inclusive DIS asymmetries A_1^h and A_1. Given that the resummed exponents are identical for the spin-averaged and spin-dependent structure functions, we expect the resummation effects to be generally very modest. On the other hand, it is also clear that the effects will not cancel identically in the spin asymmetries: even though the resummed exponents for g_1 and F_1 are identical in Mellin-moment space, they are convoluted with different parton distributions and hence no longer give identical results after Mellin inversion. Moreover, the matching procedure also introduces differences since the NLO coefficient functions are somewhat different for g_1 and F_1. It is therefore still relevant to investigate the impact of resummation on the spin asymmetries. We will compare our results to data sets from HERMES [2] and COMPASS [3,5]. In addition, we present some results relevant for measurements at the Jefferson Laboratory [6,7], in particular those to be carried out in the near future after the CEBAF upgrade to 12 GeV [12].

For our calculations we use the NLO polarized parton distribution functions of Ref. [9] and the unpolarized ones of Ref. [28]. Our choice of the latter is motivated by the fact that this set was also adopted as the baseline unpolarized set in Ref. [9], so that the two sets are consistent in the sense that the same strong coupling constant is used. Additionally, in the case of SIDIS we choose the "de Florian-Sassot-Stratmann" [29] NLO set of fragmentation functions. In this work, we choose to focus only on pions in the final state. Resummation effects for other hadrons will be very similar. The factorization and renormalization scales are set to Q.

Figures 1 and 2 present comparisons of our resummed calculations with HERMES data [2] for semi-inclusive (π^+) and inclusive DIS, respectively, both off a proton target at $\sqrt{s} \approx 7.25$ GeV. The error bars show the statistical uncertainties only. For the SIDIS asymmetry, we integrate the numerator and the denominator of Eq. (2) separately over a region of $0.2 < z < 0.8$. We plot the theoretical results at the average values of x and Q^2 of each data point and connect the points by a line. The figures show the NLO (dashed lines) and the resummed-matched (solid lines) results. As one can see, the higher-order effects generated by resummation are indeed fairly small, although not negligible. They are overall more significant for SIDIS, which is expected due to the additional threshold logarithms in SIDIS (see discussion at the end of Sec. II B). We expect the resummed results to be most reliable at rather high values of $x \gtrsim 0.2$ or so [13]. In this regime, there is a clear pattern that resummation tends

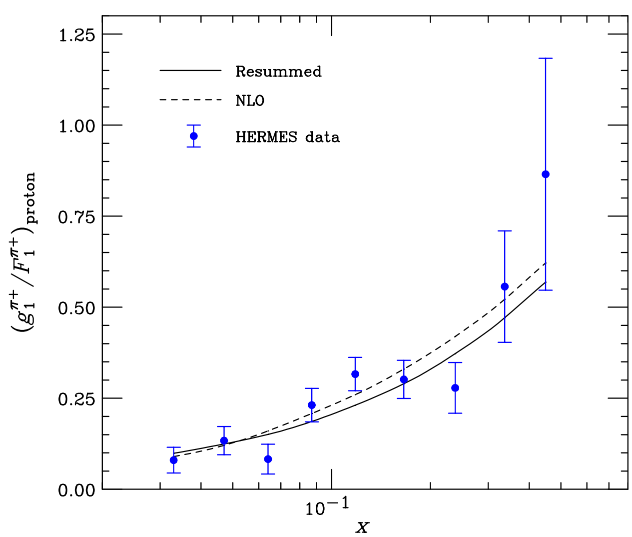

FIG. 1 (color online). Spin asymmetry for semi-inclusive π^+ production off a proton target. The data points are from Ref. [2] and show statistical errors only. The $\langle x \rangle$ and $\langle Q^2 \rangle$ values were taken according to the HERMES measurements.

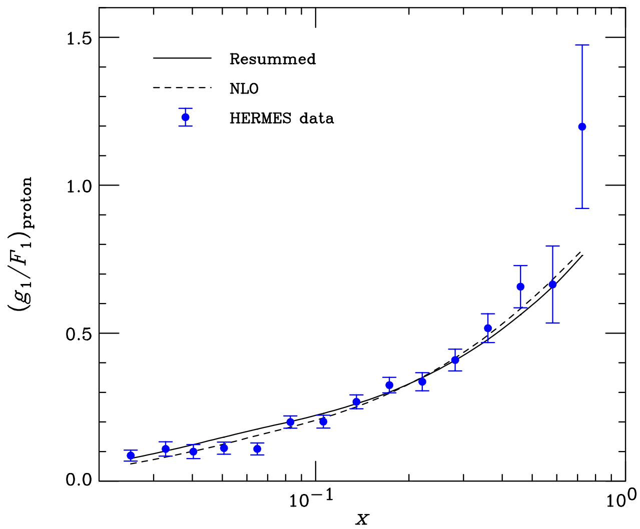

FIG. 2 (color online). Spin asymmetry for inclusive polarized DIS off a proton target. The data points are from Ref. [4] and show statistical errors only. The $\langle x\rangle$ and $\langle Q^2\rangle$ values were taken according to the HERMES measurements.

to decrease the spin asymmetries compared to NLO, more pronounced so for SIDIS. In other words, higher-order corrections enhance the spin-averaged cross section somewhat more strongly than the polarized one.

Figures 3 and 4 show similar comparisons to the SIDIS and DIS asymmetries measured by COMPASS [3,5] with a polarized muon beam at $\sqrt{s} \approx 17.4$ GeV. For COMPASS kinematics the effects of threshold resummation are overall somewhat smaller due to the fact that one is further away from partonic threshold because of the higher center-of-mass energy. However, the results remain qualitatively similar to what we observed for HERMES kinematics.

The inclusive *neutron* spin asymmetry is particularly interesting from the point of view of resummation, since

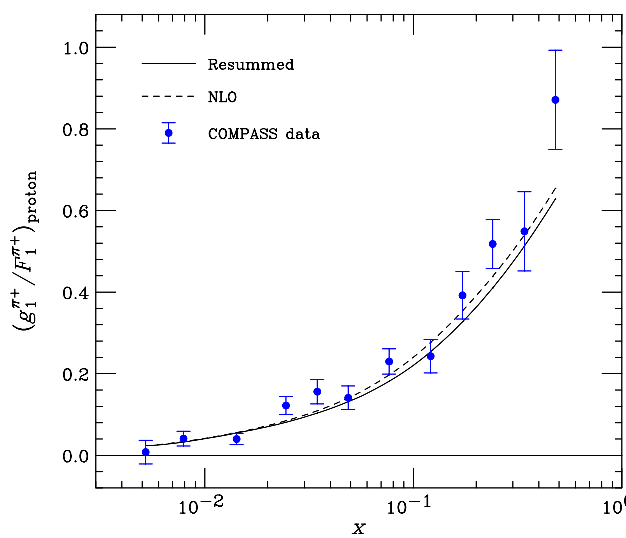

FIG. 3 (color online). Same as Fig. 1 but comparing to the COMPASS measurements [3].

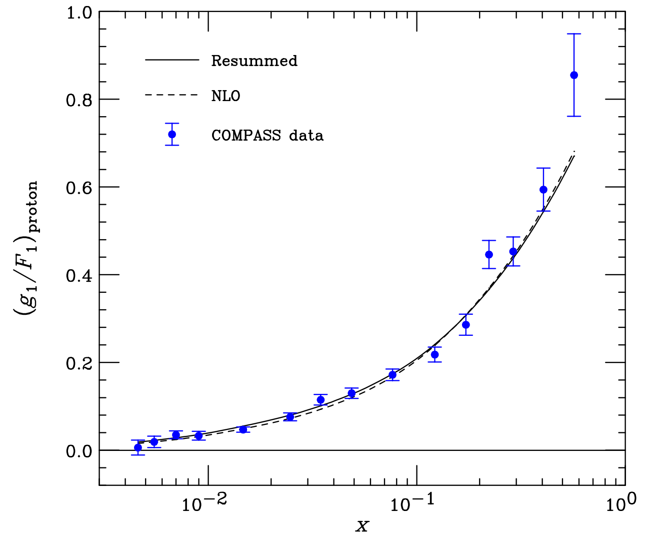

FIG. 4 (color online). Same as Fig. 2 but comparing to the COMPASS measurements [5].

it is known [6] to exhibit a sign change at fairly large values of x. Near a zero of the polarized cross section resummation effects are expected to be particularly relevant. Figure 5 shows the asymmetry at NLO and for the NLL resummed case. For illustration we show the presently most precise data available, which are from the Hall-A Collaboration [6] at the Jefferson Laboratory. In order to mimic the correlation of x and Q^2 for the present Jefferson Lab kinematics, we choose $Q^2 = x \times 8$ GeV^2 in the theoretical calculation. As one can see, the effects of resummation are indeed more pronounced than for the inclusive proton structure functions considered in Figs. 2 and 4. Evidently the zero of the asymmetry shifts slightly due to

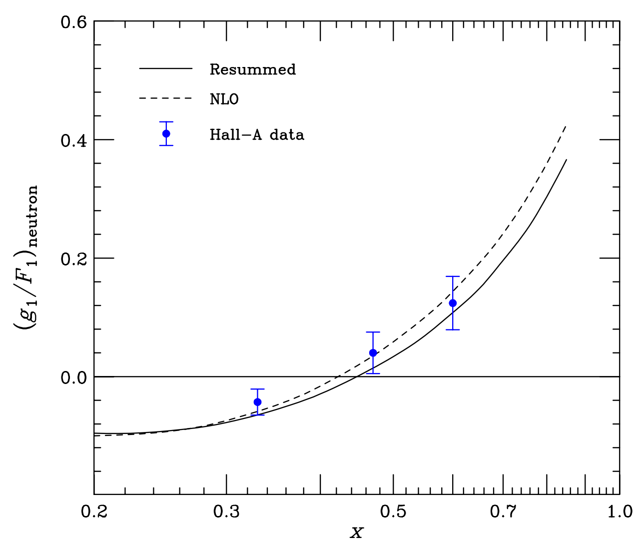

FIG. 5 (color online). Spin asymmetry for inclusive polarized DIS off a neutron target. The data points are from Ref. [6] and show statistical errors only. The Q^2 values in the theoretical calculation were chosen as $Q^2 = x \times 8$ GeV^2.

resummation. On the other hand, the asymmetry is overall still quite stable with respect to the resummed higher-order corrections.

The latter observation is quite relevant for the extraction of polarized large-x parton distributions from data for proton and neutron spin asymmetries in lepton scattering. For instance, to good approximation [6] one may use the inclusive structure functions to directly determine the combinations $(\Delta u + \Delta\bar{u})/(u + \bar{u})$ and $(\Delta d + \Delta\bar{d})/(d + \bar{d})$. At lowest order, and neglecting the contributions from strange and heavier quarks and antiquarks, one has

$$R_u \equiv \frac{\Delta u + \Delta\bar{u}}{u + \bar{u}}(x, Q^2) = \frac{4g_{1,\mathrm{p}} - g_{1,\mathrm{n}}}{4F_{1,\mathrm{p}} - F_{1,\mathrm{n}}}(x, Q^2),$$
$$R_d \equiv \frac{\Delta d + \Delta\bar{d}}{d + \bar{d}}(x, Q^2) = \frac{4g_{1,\mathrm{n}} - g_{1,\mathrm{p}}}{4F_{1,\mathrm{n}} - F_{1,\mathrm{p}}}(x, Q^2), \tag{25}$$

where the subscripts p, n denote a proton or neutron target, respectively. One may therefore determine $(\Delta u + \Delta\bar{u})/(u + \bar{u})$ and $(\Delta d + \Delta\bar{d})/(d + \bar{d})$ directly from experiment by using measured structure functions $g_{1,\mathrm{p}}$, $g_{1,\mathrm{n}}$, $F_{1,\mathrm{p}}$, $F_{1,\mathrm{n}}$ in Eq. (25). Up to certain refinements required by the fact that measurements of the ratios $g_{1,\mathrm{p}}/F_{1,\mathrm{p}}$ and $g_{1,\mathrm{n}}/F_{1,\mathrm{n}}$ are more readily available than those of the individual structure functions, this is essentially the approach used by the Hall-A Collaboration (alternatively, one may also use the corresponding spin asymmetry for the deuteron instead of the neutron one [7]). In the following we explore the typical size of the corrections to the ratios due to higher orders. Figure 6 shows first of all the structure function ratios on the right-hand side of Eq. (25), computed at NLO using as before the polarized and unpolarized parton distribution functions of Refs. [9,28], respectively (solid lines). We have again chosen $Q^2 = x \times 8\ \mathrm{GeV}^2$. Using Eq. (25), these ratios would correspond to the "direct experimental determinations" of R_u and R_d. The dashed lines in the figure show the actual ratios $(\Delta u + \Delta\bar{u})/(u + \bar{u})$ and $(\Delta d + \Delta\bar{d})/(d + \bar{d})$ as given by the sets of parton distribution functions that we use. Any difference between the solid and dashed lines is, therefore, a measure of the significance of effects related to strange quarks and antiquarks, and to NLO corrections. As one can see, these have a relatively modest size. Finally, we estimate the potential effect of resummation on R_u, R_d: following Refs. [30,31], we define "resummed" quark (and antiquark) distributions by demanding that their contributions to the structure functions g_1, F_1 match those of the corresponding NLO distributions, which is ensured by setting

$$\tilde{q}^{\,N,\mathrm{res}}(Q^2) \equiv \frac{\tilde{C}_q^{\mathrm{NLO}}(N, \alpha_s(Q^2))}{\tilde{C}_q^{\mathrm{res}}(N, \alpha_s(Q^2))}\,\tilde{q}^{N,\mathrm{NLO}}(Q^2) \tag{26}$$

in Mellin-moment space. Here, $\tilde{C}_q^{\mathrm{NLO}}$ and $\tilde{C}_q^{\mathrm{res}}$ are the NLO and resummed quark coefficient functions for the inclusive structure function F_1, respectively. We match the resummed coefficient function to the NLO one by subtracting out its NLO contribution and adding the full NLO one, in analogy with Eq. (22). Equation (26) can be straightforwardly extended to the spin-dependent case. The ratios R_u, R_d for these "resummed" parton distributions are shown by the dotted lines in Fig. 6. As one can see, they are quite close to the other results, indicating that resummation is not likely to induce very large changes in the parton polarizations extracted from future high-precision data. For illustration, we also show the Hall-A [6] and CLAS [7] data in the figure, which have been obtained using parton-model relations for the inclusive structure functions, similar to Eq. (25). One can see that the error bars of the data are presently still larger than the differences between our various theoretical results. This situation is expected to be improved with the advent of the Jefferson Lab 12-GeV upgrade [12] or an Electron Ion Collider [32]. As is well known, SIDIS measurements provide additional information on R_u, R_d, albeit so far primarily at lower x [2].

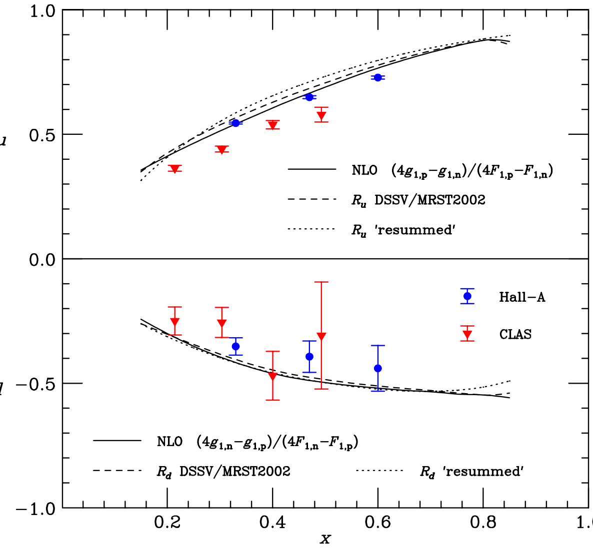

FIG. 6 (color online). High-x up and down polarizations $(\Delta u + \Delta\bar{u})/(u + \bar{u})$ and $(\Delta d + \Delta\bar{d})/(d + \bar{d})$. The solid lines show the ratios of structure functions on the right-hand sides of Eq. (25), while the dashed lines show the actual parton distribution ratios as represented by the NLO sets of Refs. [9,28]. The dotted lines show the expected shift of the distributions when resummation effects are included in their extraction, using Eq. (26). The Q^2 values in the theoretical calculation were chosen as $Q^2 = x \times 8\ \mathrm{GeV}^2$. We also show the present Hall-A [6] and CLAS [7] data obtained from inclusive DIS measurements. Their error bars are statistical only.

IV. CONCLUSIONS

We have investigated the size of threshold resummation effects on double-longitudinal spin asymmetries for inclusive and semi-inclusive deep inelastic scattering in fixed-target experiments. Overall, the asymmetries are rather stable with respect to resummation, in particular for the inclusive case. Towards large values of x, resummation tends to cause a decrease of the spin asymmetries, which is more pronounced in the semi-inclusive case and for asymmetries measured off neutron targets.

The relative robustness of the spin asymmetries bodes well for the extraction of high-x parton polarizations $(\Delta u + \Delta\bar{u})/(u + \bar{u})$ and $(\Delta d + \Delta\bar{d})/(d + \bar{d})$, which are consequently also rather robust. Nevertheless, knowledge of the predicted higher-order corrections should be quite relevant when future high-statistics large-x data become available. On the theoretical side, it will be interesting to study the interplay of our perturbative corrections with power corrections that are ultimately also expected to become important at high x [14,15,33–35], although it appears likely that present data are in a window where the perturbative corrections clearly dominate. Finally, we note that related large-x logarithmic effects have also been investigated for the nucleon's light-cone wave function [36], where they turn out to enhance components of the wave function with nonzero orbital angular momentum, impacting the large-x behavior of parton distributions. It will be very worthwhile to explore the possible connections between the logarithmic corrections discussed here and in Ref. [36].

ACKNOWLEDGMENTS

We thank Marco Stratmann for useful communications. This work was supported in part by the German Bundesministerium für Bildung und Forschung (BMBF), Grant No. 05P12VTCTG.

[1] L. L. Frankfurt, M. I. Strikman, L. Mankiewicz, A. Schafer, E. Rondio, A. Sandacz, and V. Papavassiliou, Phys. Lett. B **230**, 141 (1989).

[2] A. Airapetian *et al.* (HERMES Collaboration), Phys. Rev. D **71**, 012003 (2005).

[3] M. G. Alekseev *et al.* (COMPASS Collaboration), Phys. Lett. B **693**, 227 (2010).

[4] A. Airapetian *et al.* (HERMES Collaboration), Phys. Rev. D **75**, 012007 (2007).

[5] M. G. Alekseev *et al.* (COMPASS Collaboration), Phys. Lett. B **690**, 466 (2010).

[6] X. Zheng *et al.* (Jefferson Lab Hall A Collaboration), Phys. Rev. Lett. **92**, 012004 (2004); Phys. Rev. C **70**, 065207 (2004). See references therein for other data on the neutron spin asymmetry.

[7] K. V. Dharmawardane *et al.* (CLAS Collaboration), Phys. Lett. B **641**, 11 (2006).

[8] For a review of the earlier DIS and SIDIS data, see M. Burkardt, C. A. Miller, and W. D. Nowak, Rep. Prog. Phys. **73**, 016201 (2010).

[9] D. de Florian, R. Sassot, M. Stratmann, and W. Vogelsang, Phys. Rev. Lett. **101**, 072001 (2008); Phys. Rev. D **80**, 034030 (2009).

[10] D. de Florian, R. Sassot, M. Stratmann, and W. Vogelsang, arXiv:1108.3955.

[11] E. Leader, A. V. Sidorov, and D. B. Stamenov, Phys. Rev. D **82**, 114018 (2010).

[12] V. D. Burkert, arXiv:1203.2373.

[13] D. P. Anderle, F. Ringer, and W. Vogelsang, Phys. Rev. D **87**, 034014 (2013).

[14] S. Simula, M. Osipenko, G. Ricco, and M. Taiuti, Phys. Rev. D **65**, 034017 (2002).

[15] M. Osipenko, S. Simula, W. Melnitchouk, P. E. Bosted, V. Burkert, E. Christy, K. Griffioen, C. Keppel, S. Kuhn, and G. Ricco, Phys. Rev. D **71**, 054007 (2005).

[16] D. de Florian, M. Stratmann, and W. Vogelsang, Phys. Rev. D **57**, 5811 (1998).

[17] D. de Florian and Y. R. Habarnau, Eur. Phys. J. C **73**, 2356 (2013).

[18] G. Altarelli, R. K. Ellis, G. Martinelli, and S. Y. Pi, Nucl. Phys. **B160**, 301 (1979).

[19] P. Nason and B. R. Webber, Nucl. Phys. **B421**, 473 (1994); **B480**, 755(E) (1996).

[20] W. Furmanski and R. Petronzio, Z. Phys. C **11**, 293 (1982).

[21] D. Graudenz, Nucl. Phys. **B432**, 351 (1994).

[22] M. Glück, E. Reya, M. Stratmann, and W. Vogelsang, Phys. Rev. D **53**, 4775 (1996).

[23] G. F. Sterman and W. Vogelsang, Phys. Rev. D **74**, 114002 (2006).

[24] For related work, see also M. Cacciari and S. Catani, Nucl. Phys. **B617**, 253 (2001).

[25] M. Stratmann and W. Vogelsang, Phys. Rev. D **64**, 114007 (2001).

[26] S. Catani, M. L. Mangano, P. Nason, and L. Trentadue, Nucl. Phys. **B478**, 273 (1996).

[27] S. Catani, M. L. Mangano, and P. Nason, J. High Energy Phys. 07 (1998) 024.

[28] A. D. Martin, R. G. Roberts, W. J. Stirling, and R. S. Thorne, Eur. Phys. J. C **28**, 455 (2003).

[29] D. de Florian, R. Sassot, and M. Stratmann, Phys. Rev. D **75**, 114010 (2007).

[30] G. F. Sterman and W. Vogelsang, arXiv:hep-ph/0002132.

[31] G. Corcella and L. Magnea, Phys. Rev. D **72**, 074017 (2005).

[32] E. C. Aschenauer, R. Sassot, and M. Stratmann, Phys. Rev. D **86**, 054020 (2012).

[33] E. Leader, A. V. Sidorov, and D. B. Stamenov, Phys. Rev. D **75**, 074027 (2007); **80**, 054026 (2009).

[34] J. Blümlein and H. Böttcher, Nucl. Phys. **B841**, 205 (2010).

[35] A. Accardi and W. Melnitchouk, Phys. Lett. B **670**, 114 (2008); A. Accardi, T. Hobbs, and W. Melnitchouk, J. High Energy Phys. 11 (2009) 084; L. T. Brady, A. Accardi, T. J. Hobbs, and W. Melnitchouk, Phys. Rev. D **84**, 074008 (2011); **85**, 039902(E) (2012).

[36] H. Avakian, S. J. Brodsky, A. Deur, and F. Yuan, Phys. Rev. Lett. **99**, 082001 (2007).